JACS
JOURNAL OF THE AMERICAN CHEMICAL SOCIETY
Article
pubs.acs.org/JACS

Catalysis in a Porous Molecular Capsule: Activation by Regulated Access to Sixty Metal Centers Spanning a Truncated Icosahedron

Sivil Kopilevich,[†] Adrià Gil,[‡] Miquel Garcia-Ratés,[§] Josep Bonet-Ávalos,[§] Carles Bo,[‡] Achim Müller,[∥] and Ira A. Weinstock*,[†]

[†]Department of Chemistry and the Ilse Katz Institute for Nanoscale Science and Technology, Ben Gurion University of the Negev, Beer Sheva, 84105, Israel

[§]Department of Chemical Engineering, ETSEQ, Universitat Rovira i Virgili, Tarragona, 43007, Spain

[‡]Institute of Chemical Research of Catalonia, ICIQ, Tarragona, 43007, Spain

[∥]Faculty of Chemistry, University of Bielefeld, Bielefeld, D-33501, Germany

Supporting Information

ABSTRACT: The 30 cationic $\{Mo^{V}_{2}O_{4}(acetate)\}^{+}$ units linking 12 negatively charged pentagonal "ligands," $\{(Mo^{VI})Mo^{VI}_{5}O_{21}(H_2O)_6\}^{6-}$ of the porous metal-oxide capsule, $[\{Mo^{VI}_{6}O_{21}(H_2O)_6\}_{12}\{Mo^{V}_{2}O_{4}(acetate)\}_{30}]^{42-}$ provide active sites for catalytic transformations of organic "guests". This is demonstrated using a well-behaved model reaction, the fully reversible cleavage and formation of methyl *tert*-butyl ether (MTBE) under mild conditions in water. Five independent lines of evidence demonstrate that reactions of the MTBE guests occur in the ca. 6×10^3 Å^3 interior of the spherical capsule. The Mo atoms of the $\{Mo^{V}_{2}O_{4}(acetate)\}^{+}$ linkers—spanning an ca. 3-nm truncated icosahedron—are sterically accessible to substrate, and controlled removal of their internally bound acetate ligands generates catalytically active $\{Mo^{V}_{2}O_{4}(H_2O)_2\}^{2+}$ units with labile water ligands, and Lewis- and Brønsted-acid properties. The activity of these units is demonstrating by kinetic data that reveal a first-order dependence of MTBE cleavage rates on the number of acetate-free $\{Mo^{V}_{2}O_{4}(H_2O)_2\}^{2+}$ linkers. DFT calculations point to a pathway involving both Mo(V) centers, and the intermediacy of isobutene in both forward and reverse reactions. A plausible catalytic cycle—satisfying microscopic reversibility—is supported by activation parameters for MTBE cleavage, deuterium and oxygen-18 labeling studies, and by reactions of deliberately added isobutene and of a water-soluble isobutene analog. More generally, pore-restricted encapsulation, ligand-regulated access to *multiple* structurally integral metal-centers, and options for modifying the microenvironment within this new type of nanoreactor, suggest numerous additional transformations of organic substrates by this and related molybdenum-oxide based capsules.

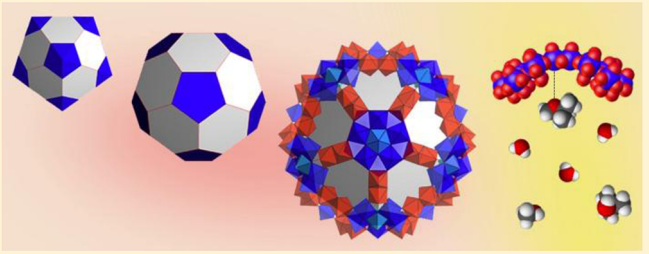

INTRODUCTION

The rational design of self-assembled structures based on the ligand-directing properties of metal cations and the dimensions and binding motifs of bridging ligands has generated a large library of one-, two-, and three-dimensional coordination polymers.[1] Among these are numerous supramolecular structures that serve as "hosts" for a variety of molecular "guests". The chemically unique and spatially restricted environments inside these host structures can accelerate reactions of guest substrates, stabilize reactive intermediates, and lead to enhanced selectivities and novel stereochemical outcomes.[2] In many cases, catalysis is achieved through hydrophobic and/or electrostatic interactions, involving both substrates and host complexes, and in others, organometallic catalysts are noncovalently bound inside the frameworks. Generally, however, the *structurally integrated*, and typically *low-valent* late-transition metals used in the coordination-driven self-assembly of these capsules are not directly involved in reactions with guest substrates.

We now report that ligand-regulated access to *multiple structurally integrated high-valent* (formally) Mo(V) centers of a porous molybdenum-oxide capsule with approximately icosahedral- (I_h) symmetry (Figure 1), results in catalysis of a model organic reaction in water, the fully reversible cleavage and formation of methyl *tert*-butyl ether (MTBE).

The representative complex used in this work, $Na_{34}[\{Mo^{VI}_{6}O_{21}(H_2O)_6\}_{12}\{(Mo^{V}_{2}O_{4})_{30}(OAc)_{22}(H_2O)_{16}\}]\cdot \sim 300H_2O$ (abbreviated as Na_{34}**1** · ca. 300 H_2O),[4a] belongs to a family of molecular metal-oxide-based coordination polymers with spherical periodicity (see ref 3a for the definition), in which 12 (formally) negatively charged pentagonal "ligands", $\{(Mo^{VI})Mo^{VI}_{5}O_{21}(H_2O)_6\}^{6-}$, are linked by 30 cationic $V^{IV}O^{2+}$, Cr^{3+}, Fe^{3+}, or $Mo^{V}_{2}O_{4}^{2+}$ "spacers",[3] giving I_h-symmetry structures of the metal skeletons. Compound **1** (Figure 1) contains 30 $Mo^{V}_{2}O_{4}^{2+}$ linkers, abbreviated $\{Mo^{V}_{2}\}$, 22 of which

Received: May 9, 2012

   dx.doi.org/10.1021/ja304513t | J. Am. Chem. Soc. XXXX, XXX, XXX–XXX

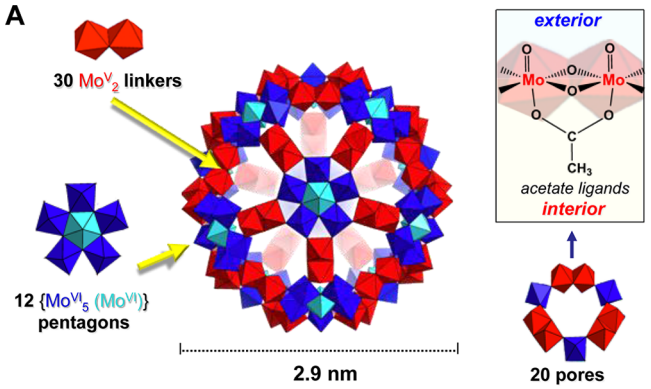

Figure 1. Structure of **1**. Mo(VI) atoms are shown in blue and green, and Mo(V) atoms in red. Exchangeable acetate ligands are bound to the interior of the capsule by bidentate coordination to 22 of the {Mo^{V}_2} linkers.

are coordinated by *labile* acetate ligands bound in a bidentate fashion to the two Mo centers, with the remaining 8 {Mo^{V}_2} units each occupied by two labile H_2O ligands. Coordination of the 12 pentagonal "ligands" to the 30 {Mo^{V}_2} linkers creates 20 Mo_9O_9 rings, 3.2 Å in diameter based on the van der Waals radii of opposing O atoms. These flexible[4a,c] rings serve as pore-like openings to the interior of the water-soluble capsules.

RESULTS AND DISCUSSION

Reversible Cleavage of methyl *tert*-butyl ether (MTBE). The ^{1}H NMR spectrum of the Na^+ salt of **1** is shown in Figure 2; see figure caption for assignments.[4a,b] The

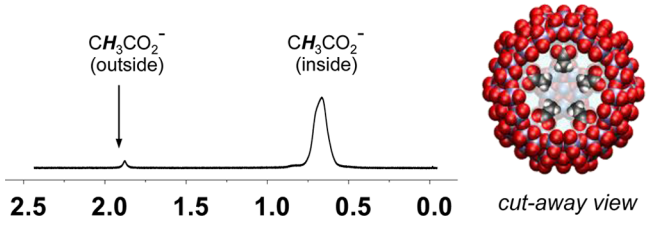

Figure 2. The ^{1}H NMR spectrum of **1** (in D_2O) shows a broad signal of the internally bound acetate ligands (illustrated in the inset), in dynamic equilibrium with those in solution outside the capsule (1.8 ppm).

signal arising from the methyl protons of the acetate ligands inside the capsule is shifted to lower-frequency (smaller) chemical shift values, as is typical for encapsulations of carboxylate ligands inside 1,[4] and of other guests such as aliphatic alcohols that do not bind to the Mo(V) centers.[4d] Characteristic broad signals arise from encapsulating guests in large macromolecules, which influences the relevant relaxation times, T_1 and especially T_2.

Hydrophobic effects are known to result in the uptake of several equivalents *n*-butanol by a propionate-ligand form of the capsule,[4d] and by **1** (this work). Apart from the presence of the acetate ligands, these effects provide a driving force for the uptake of MTBE. The entry of MTBE may also result (at least in part) from the concentration gradient established upon its addition to solutions of **1**.

Nevertheless, at room temperature, diffusion of MTBE into **1** through the smaller yet flexible Mo_9O_9 pores is slow. The rates at which organic guests enter the capsule are controlled by the size and flexibility of the Mo_9O_9 pores. In solid-state oxides, the entry of substrates larger than the sizes of the rigid pores in those materials is effectively blocked. In solutions of **1**, however, the pores of the molecular capsule are considerably more flexible, allowing the passage of guests larger than the crystallographic dimensions of the pores.[4a]

After 24 h, ca. 0.5 equiv. of MTBE is encapsulated, as indicated by broad signals at 1.7 and −0.2 ppm, assigned to $-CH_3$ and $-C(CH_3)_3$, respectively. No MeOH is observed. After 12 days (Figure 3A), 1.4 equiv. of MTBE are present

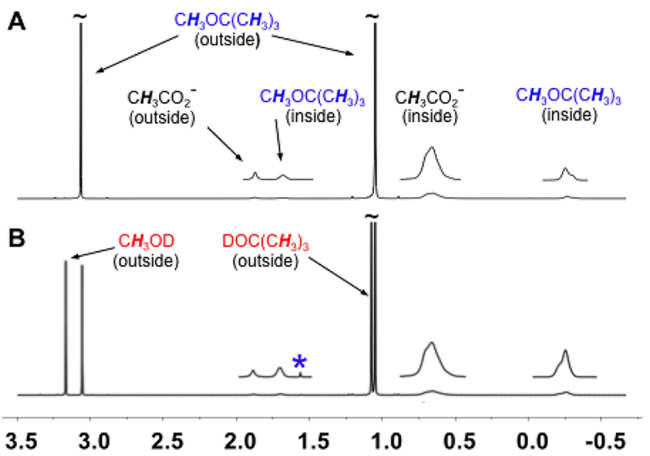

Figure 3. Encapsulation and cleavage of MTBE by **1**. **A**: H-1 NMR spectra of **1** (3.6 mM) and MTBE (182 mM) after 12 days at room temperature. The signals due to the acetate ligands (insets) are small relative to those from MTBE; 1.4 equiv. of encapsulated MTBE give rise to broad signals at 1.7 and −0.2 ppm. **B**: After 44 h at 65 °C, MeOD and *tert*-BuOH (ca. 50% conversion), are observed in the bulk solution outside the capsule, and a new sharp signal 1.6 ppm, due to an isobutene intermediate (discussed later), is indicated by an asterisk.

inside **1**, and traces of MeOH and *tert*-BuOH are observed. Once heated to 65 °C, however, the concentration of MTBE inside **1** increases rapidly, reaching ca. 4.5 equiv. after 24 h, and *tert*-BuOH (TBA) and MeOD are observed (eq 1); a representative spectrum (ca. 50% conversion after 44 h at 65 °C) is shown in Figure 3B.

$$tert\text{-BuOMe} + D_2O \rightleftharpoons tert\text{-BuOD} + MeOD \quad (1)$$

In control experiments involving both MTBE and pH 4.5 acetate buffer, only a trace amount of methanol (0.1% conversion) was observed after 24 h at 65 °C, compared to 25.5% conversion in the presence of **1** at the concentrations used in Figure 3. These values indicate that the initial rate of MTBE cleavage in the presence of **1** is >200 times that for the control.

The formation of MTBE from *tert*-BuOH and MeOH, and the reversibility of the cleavage reaction in eq 1 were simultaneously established by carrying out parallel experiments in two NMR tubes, each containing identical volumes of 3.6 mM solutions of **1** in D_2O. One contained MTBE (182 mM), and the second, a 1:1 mixture of *tert*-BuOH and MeOH (Figure S1 of the Supporting Information, SI). Both tubes were flame-sealed to avoid evaporative loss of MTBE (bp 55.2 °C). After ca. 12 days (288 h) at 65 °C, both solutions contained the *same concentrations of all three species* (Figure 4). These concentrations gave an equilibrium constant, *K*, for the cleavage reaction in eq 1 of 18 ± 1 M, from which, ΔG° (at 338K) = −1.94 ± 0.04 kcal mol^{-1}.

dx.doi.org/10.1021/ja304513t | J. Am. Chem. Soc. XXXX, XXX, XXX–XXX

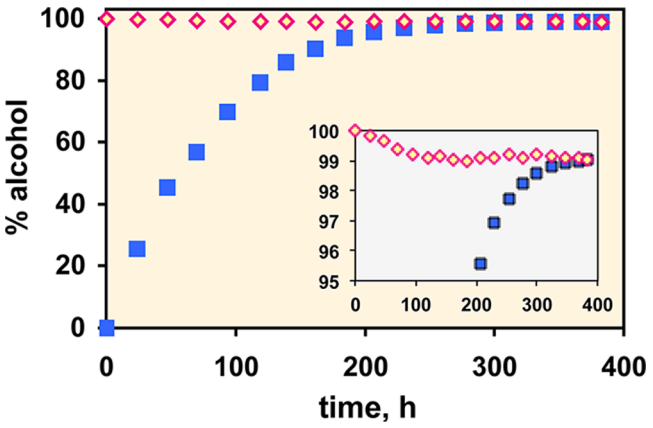

Figure 4. Cleavage of MTBE to *tert*-BuOD and MeOD (blue squares), and its reverse, the formation of MTBE (red diamonds) from *tert*-BuOD and MeOD at 65 °C in D_2O. At equilibrium, the ratio of MTBE to MeOD is 1:99; see inset.

For ether cleavage (blue squares in Figure 4), the *initial* turnover rate (i.e., far from equilibrium) was ~1 h^{-1}, and equilibrium was reached after ~50 turnovers. (No decomposition of **1** was detected by ^{1}H NMR; see Figure S2 of the SI.[4c])

Rate Expression for MTBE Cleavage. Given the small equilibrium concentration of MTBE, the progress of the cleavage reaction can be closely approximated by treating the rate of ether cleavage to 90% completion as an exponential function of [MTBE], eq 2. Using eq 2, the linear plot in Figure 5A shows that the cleavage reaction is first order in [MTBE], with $k_{obs} = k\cdot[\mathbf{1}]$.

$$\ln([\mathrm{MTBE}]/[\mathrm{MTBE}]_0) = -k_{obs}\cdot t \quad (2)$$

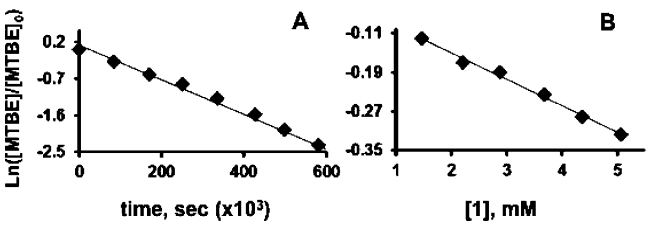

Figure 5. Kinetic plots showing that MTBE cleavage is first order in [MTBE] (**A**) and in [**1**] (**B**). Data in **A** are from Figure 4 (blue squares); data in **B** were obtained by quantifying MTBE cleavage in reactions with incrementally larger concentrations of **1**.

The dependence of rate on the concentration of **1** was evaluated by measuring the percent conversion of MTBE to *tert*-BuOH and MeOD. For this, initial concentrations of MTBE, $[\mathrm{MTBE}]_0$, were kept constant in a series of reactions involving incrementally larger concentrations of **1**. Final concentrations of MTBE, [MTBE], were determined by ^{1}H NMR after 14.5 h. The linear dependence of $\ln[\mathrm{MTBE}]/[\mathrm{MTBE}]_0$ on [**1**] in Figure 5B shows that ether cleavage is first order in [**1**].

These data give the rate expression for ether cleavage shown in eq 3, where, *from both plots in* Figure 5, $k = 1.07 \pm 0.04 \times 10^{-3}$ M^{-1} s^{-1}.

$$-\mathrm{d}[\mathrm{MTBE}]/\mathrm{dt} = k[\mathrm{MTBE}][\mathbf{1}] \quad (3)$$

Evidence for Reaction Inside 1. The first-order dependence of rate on both [**1**] and [MTBE] establishes that MTBE cleavage is catalyzed by **1**. Five lines of evidence were then used to demonstrate that ether cleavage occurs *inside* the capsule, rather than on its exterior surface.

First, MTBE was reacted with the isopolymolybdates (predominantly heptamolybdate, $[Mo_7O_{24}]^{6-}$) obtained by acidification of Na_2MoO_4 (final concentration 0.41 M) to pH 4.5 by acetic acid. Only trace amounts of methanol were observed after 24 h at 65 °C. Moreover, no MeOH was detected after refluxing MTBE in an aqueous solution of the bis-(triphenylphosphine)iminium salt of MoO_4^{2-}.[5]

Second, when the size of the substrate was modestly increased by changing the methyl group on oxygen to ethyl (**B** in Chart 1), conversion after 24 h at 65 °C decreased from

Chart 1. MTBE and Two Larger Derivatives

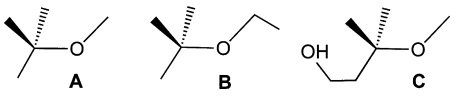

25 to 14% (concentrations used were the same as those in Figure 3). After adding a $-CH_2OH$ group to the already large *tert*-butyl group of MTBE, to give 3-methyl-3-methoxy-butanol (**C**), much less of the substrate was encapsulated (ca. 2 equiv. after 24 h 65 °C), and conversion dropped to 7%.

A third line of evidence was provided by replacing acetate ligands in **1** by 12 equiv. of benzoate (Figure 6; an ^{1}H NMR

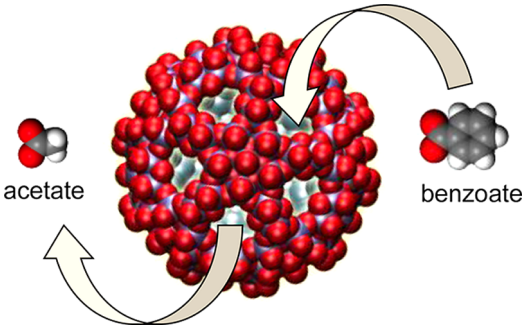

Figure 6. Partial replacement of interior acetate ligands by 12 benzoate ligands inhibits the entry of MTBE and dramatically decreases the rate of MTBE cleavage.

spectrum is provided in Figure S3 of the SI),[6] so that the *larger ligands* might inhibit access of MTBE to the capsule's interior. MTBE-cleavage was then carried out under the same conditions as those used in Figure 3. After 24 h, the amount of MTBE discernible by ^{1}H NMR inside the capsule was small, *and an order-of-magnitude less MeOD was produced*: ca. 2% conversion, compared to 25%.

Molecular dynamics simulations confirmed that the hydrophobic benzoate ligands are less labile than are acetate ligands in **1**, and decrease the amount of water inside the capsule (see the SI). This unique microenvironment, along with steric effects, both inhibit the entry of MTBE into the capsule.

A fourth line of evidence was provided by using **1** to catalyze the cleavage of *p*-dimethoxybenzene (*p*-DMB) (Figure 7). Upon heating to 65 °C in D_2O, MeOD was observed in the bulk solution outside the capsule, while the (larger) phenolic

dx.doi.org/10.1021/ja304513t | J. Am. Chem. Soc. XXXX, XXX, XXX–XXX

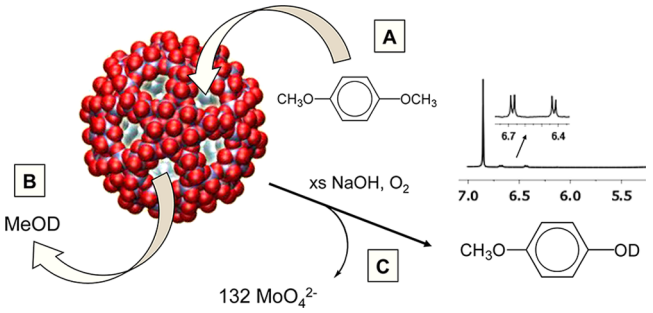

Figure 7. Upon cleavage of *p*-dimethoxybenzene (*p*-DMB), the larger product is initially "trapped" inside the capsule. **A**: *p*-DMB is encapsulated by **1**; **B**: Initially, MeOD is the only product observed by ^{1}H NMR in bulk solution outside **1**; **C**: *p*-Methoxyphenol (*p*-MP), whose rate of egress is much slower than that of MeOD, was identified by ^{1}H NMR (inset) after "cracking open" the capsule (NaOH and O_2). Control experiments ruled out the formation of *p*-MP during the oxidative hydrolysis of **1**. (See Figures S4–S8 of the SI for ^{1}H NMR spectra related to all three stages.)

product, *p*-methoxyphenol (*p*-MP) was initially observed *exclusively inside* **1**.

A fifth and highly informative line of evidence was obtained after further analysis of the rate constant, *k*, in eq 3. Namely, after reacting MTBE (182 mM) with **1** (3.6 mM) for 3 h at 65 °C, the concentration of MTBE inside **1** was *6 times* that of MeOD. Hence, the entry of MTBE through the Mo_9O_9 pores of **1** is not rate limiting, such that *k* (eq 3) must refer to ether cleavage *inside* the capsule. Having established this, it was possible to determine whether rate constants for MTBE cleavage varied as the number of $\{Mo^V_2\}$ linkers occupied by water versus acetate ligands was systematically varied.

For this, a series of capsules was prepared in which internal acetate ligands were incrementally replaced by water (two per $\{Mo^V_2\}$ unit). Rate constants for MTBE cleavage were then found to increase linearly with the number of water-bound $\{Mo^V_2\}$ linkages (Figure 8). This not only proves that MTBE

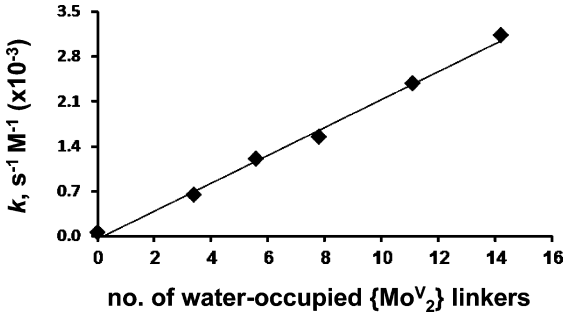

Figure 8. Effect of the number of "available" (water-bound) $\{Mo^V_2\}$ linkers on rate constants for MTBE cleavage. The plot includes a correction to the *x*-axis; see additional data and discussion of this procedure in the SI.

cleavage occurs inside **1**, but also reveals that catalysis occurs exclusively at the hydrated $\{Mo^V_2\}$ linkers, $\{Mo^V_2O_4(H_2O)_2\}^{2+}$, rather than under the $\{(Mo^{VI})Mo^{VI}_5O_{21}(H_2O)_6\}^{6-}$ pentagons. More generally, it shows that access of substrates to Mo(V) active sites inside **1** can be deliberately regulated by varying the number of internally bound carboxylate ligands.

When organic ligands are combined with small numbers of transition-metal ions to give, e.g., T_d- and O_h-symmetry coordination polymers, the restricted internal dimensions of those capsules inhibit the access of substrates to the metal cations. The ca. 6×10^3 Å^3 interior of **1** is substantially larger, however, such that MTBE can readily access the $\{Mo^V_2\}$ units that span the capsule's I_h-symmetry metal-oxide skeleton.

Reaction Mechanism. Information about the mechanism of catalysis at the $\{Mo^V_2\}$ linkers was provided by MTBE cleavage in ^{18}O-labeled H_2O. As shown in eq 4, the ^{18}O label

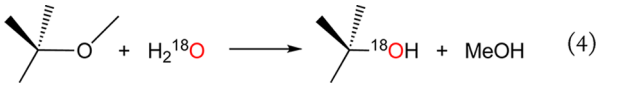

was found exclusively on *tert*-BuOH (by GC MS; Figures S10 and S11 of the SI). Hence, MTBE hydrolysis occurs exclusively via cleavage of the Me_3C-O bond, ruling out an associative mechanism involving (sterically difficult) nucleophilic attack on the *tert*-butyl group.

At this juncture, DFT calculations (Figures S12–S14 of the SI) indicated that the (formal) elimination of methanol from MTBE to give an olefinic intermediate, isobutene, would be kinetically viable if it occurred via a concerted process involving both Mo(V) atoms of each $\{Mo^V_2\}$ linker (Figure 9).

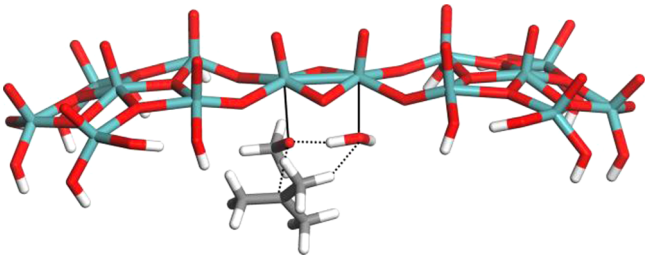

Figure 9. Proposed transition state for isobutene formation at a bifunctional $\{Mo^V_2\}$ linker. The $\{Mo^V_2\}$ unit, with Mo atoms in green, is shown between two pentagonal units, at left and right. The ether oxygen is bound to one Mo(V) atom, acting as a Lewis acid,[7a] while a water molecule on the adjacent Mo(V) atom serves as a "proton-shuttle" in a six-membered transition-state.

The proposed transition-state structure involves one Mo(V)-bound water molecule acting as a proton "shuttle", and one Mo(V) center serving as a Lewis-acid. On the basis of pD values of 3.6 mM solutions of **1** in D_2O—which vary from 3 to 5 depending on the number of internal acetate ligands present—the pK_a values of water molecules bound to Mo(V) centers are estimated at ca. 3.5 to 5.0, similar to water ligands on Ti(IV) in titanocene.[7a,b] However, the water ligands in the $\{Mo^V_2O_4(H_2O)_2\}^{2+}$ linkers are labile (have a rather short residence time): On the basis of published data,[11] exchange rates are estimated at between 10^3 and 10^5 s^{-1}.[11b]

Consistent with bond breaking in an organized transition state, the temperature dependence of the rate constant for MTBE cleavage (R^2 = 0.9998 for five temperatures) gave enthalpies and entropies of activation of $\Delta H^{\ddagger} = 21.6 \pm 0.2$ kcal mol^{-1} and $\Delta S^{\ddagger} = -8.6 \pm 0.5$ cal mol^{-1} K^{-1} (Figure 10).

The subsequent hydration of isobutene in D_2O—catalyzed by the $\{Mo^V_2\}$ linkers, but with a smaller activation energy based on DFT results—should incorporate deuterium into the methyl groups of the *tert*-BuOD product (eq 5). This was definitively confirmed by ESI MS (Figure S15 of the SI).[8]

In line with this, the small signal at 1.6 ppm consistently observed during MTBE cleavage and formation (labeled with

dx.doi.org/10.1021/ja304513t | J. Am. Chem. Soc. XXXX, XXX, XXX–XXX

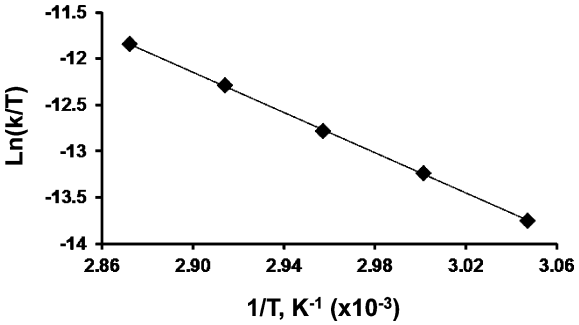

Figure 10. Eyring plot of $\ln(k/T)$ vs $1/T$ from the temperature dependence of rate constants for MTBE cleavage.

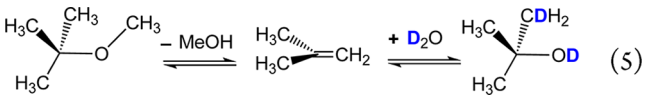

(5)

an asterisk in Figure 3B) was positively identified as isobutene. Moreover, when a water-soluble analogue, (**B** in eq 6), or the related ether or alcohol (**A** or **C**, respectively), was reacted with **1** and MeOH, *all three species* were observed by ^{1}H NMR (eq 6, shown for simplicity in H_2O).

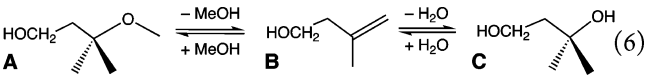

(6)

The reversible nature of MTBE cleavage (Figure 4) requires that each elementary step in the **1**-catalyzed process must be microscopically reversible. A plausible mechanistic cycle based on DFT calculations—including the transition-state structure in Figure 9—consistent with all the above findings, and that *fully satisfies microscopic reversibility*,[9] is provided in Figure S16 of the SI. The proposed mechanistic sequence, involving bifunctional (Lewis acid[7] and general acid/base[10]) sites at each $\{Mo^V_2\}$ unit, is an attractive possibility insofar as bifunctionality is a hallmark of many enzymatic processes.[2b,12]

CONCLUSIONS

In summary, the 30 $Mo^V_2O_4^{2+}$ linkers, $\{Mo^V_2\}$, that combine with the 12 negatively charged $\{(Mo^{VI})Mo^{VI}_5O_{21}(H_2O)_6\}^{6-}$ pentagonal "ligands" of a porous metal-oxide capsule are active sites for catalysis of a well-behaved model reaction, the fully reversible cleavage and formation of methyl *tert*-butyl ether. The data provided systematically demonstrate that the reactions occur in the ca. 6×10^3 Å^3 interior of the porous capsule, and that control over the number of internally bound acetate ligands can be used to generate specific numbers of catalytically active $\{Mo^V_2O_4(H_2O)_2\}^{2+}$ units. The *tert*-butyl groups of the substrate "guests" are larger than the crystallographic dimensions of the Mo_9O_9 pores through which they must pass to enter or leave the capsule,[4] and catalytic activity is a consequence of the long residence times of the relatively large substrates inside the capsule, combined with the capsule's tunable internal microenvironment.

More generally, pore-restricted encapsulation, ligand-regulated access to *multiple* structurally integral metal center based $\{Mo^V_2O_4(H_2O)_2\}^{2+}$ groups acting as both Lewis acid and general-acid/base sites, combined with ready options for modification of the internal microenvironment through the introduction of e.g., chiral, hydrophobic, and/or reactive ligands, suggest numerous additional prospects for catalytic transformations of organic substrates in water by porous molybdenum-oxide based nanocapsules.

EXPERIMENTAL SECTION

Materials and Reagents. Regenerated-cellulose dialysis membranes (45-mm flat-width tubes; 12−14 000 Da MWCO) were purchased from VWR Scientific, treated before use to remove glycerin and traces of sulfur compounds, and stored under high-purity water (17 MΩ, Millipore) at 5 °C. *tert*-Butyl methyl ether (≥99.5%; Fisher Scientific), methanol (≥99.5%; Bio Lab), 1,4-dimethoxybenzene (≥99%; Aldrich), 4-methoxyphenol (≥99%; Aldrich), deuterium oxide (≥99.9% D; CIL), ammonium acetate (ACS, Mallinckrodte), ammonium molybdate 4-hydrate (ACS; Mallinckrodte), hydrazine sulfate (≥98%; Fluka), oxygen-18 enriched water (≥98% ^{18}O; Dchem), 3-methoxy-3-methyl-1-butanol (≥98%; Aldrich), 3-methyl-3-butene-1-ol (≥97%; Aldrich), and 3-methyl-1,3-butanediol (≥97%; Aldrich) were used as received. $Na_{34}[\{Mo^{VI}_6O_{21}(H_2O)_6\}_{12}\{(Mo^V_2O_4)_{30}(OAc)_{22}(H_2O)_{16}\}]\cdot\sim 300H_2O$ (abbreviated as Na_{34}**1** · ca. 300 H_2O) was prepared as previously described.[4a] All reactions were carried out in 17 MΩ Millipore water or D_2O. All other reagents were obtained from commercial sources and used as received.

Instrumentation. pH values were measured using a EuTech pH 510 Bench-Top pH meter equipped with a Ag/AgCl electrode (Thermo Electron, U.K) and temperature compensation. A digital hot plate/stirrer MH-220 (MRC) equipped with a PT-100 sensor was used to control the oil-bath temperatures. Proton-NMR spectra were acquired on Bruker 400 and 500 MHz spectrometers, and the HDO signal in D_2O samples was used as an internal chemical-shift reference (relative to tetramethylsilane, TMS). Spectral data were processed using Mnova version 6.1. Gas chromatographic mass spectral (GCMS) data were obtained using an Agilent 6850 GC equipped with an Agilent 5973 MSD working under standard conditions and an Agilent HP5-MS column.

Internal Integration Standard. Methane sulfonic acid (MSA) (0.0183 g, 0.189 mmol) was dissolved in 3 mL of D_2O in a 5 mL volumetric flask, and neutralized using a solution of NaOH in D_2O until the pH reached 4.0. Additional D_2O was added to bring the volume to 5 mL. The final pH was 4.5 and the final concentration of MSA was 37.89 mM. This solution used as an internal standard for ^{1}H NMR.

External integration standard. Methane sulfonic acid (MSA) (0.0354 g, 3.66 mmol) was dissolved in 600 μL of D_2O. Then, 60 μL of this solution was transferred to coaxial inner cell ("micro tube"; NE-5-CIC, New Era). Sodium tetraphenylborate (TPB; 0.0250 g, 72.4 μmol) was dissolved in 5 mL D_2O. Then, 500 μL of this solution transferred to a thin walled 5-mm precision NMR tube (ML-5, New Era). The "micro tube" was inserted into the 5-mm tube, and the number of equivalents of MSA relative to tetraphenylborate was calculated from ^{1}H NMR signal-intensity ratios. To increase accuracy, the calibration was repeated using three different TPB solutions.

Kinetics and Reversible Cleavage of Methyl *tert*-Butylether (MTBE). For MTBE cleavage, 15 μL of pure MTBE were added to an NMR tube containing 1.81 μmol of Na_{34}**1** in D_2O (50 mg in 485 μL D_2O). After addition, the NMR tube was flame-sealed under air and transferred to an oil bath kept at a constant temperature of 65 °C. H-1 NMR spectra were acquired every ∼24 h. For MTBE formation, 5.1 μL MeOH and 11.8 μL of *tert*-ButOH were added to an NMR tube containing 1.81 μmol of Na_{34}**1** in D_2O (50 mg in 485 μL D_2O). After addition, the NMR tube was flame-sealed under air and transferred to an oil bath kept at a constant temperature of 65 °C. NMR spectra were acquired every ∼24 h.

MTBE Cleavage in ^{18}O-Labeled Water. The sample was prepared as immediately above, but in $H_2{}^{18}O$ rather than in D_2O, and kept at 65 °C for 120 h. The solution was then transferred to a 4 mL vial and extracted with 2 mL of ethyl acetate. The extracts were dried over $MgSO_4$, and the ^{18}O labeled products were identified by GC-MS.

dx.doi.org/10.1021/ja304513t | J. Am. Chem. Soc. XXXX, XXX, XXX−XXX

Dependence of Cleavage Rate on [Na_{34}1]. For this, 20, 30, 40, 50, 60, and 70 mg amounts of Na_{34}**1** were each dissolved in 485 μL D_2O. The solutions were transferred to separate NMR tubes, and 15 μL of pure MTBE were added to each tube. The NMR tubes were closed tightly (but not flame-sealed) and placed in an oil bath kept at a constant temperature of 65 °C. H-1 NMR spectra were acquired after 14 h 40 min.

Preparation of $Na_{37}[\{Mo^{VI}_6O_{21}(H_2O)_6\}_{12}\{(Mo^{V}_2O_4)_{30}-(OAc)_{13}(C_6H_5CO_2)_{12}(H_2O)_{10}\}]$, Abbreviated as Na_{37}1-$(CH_3CO_2)_{13}(C_6H_5CO_2)_{12}$. Two 0.1 M benzoate buffer solutions (0.5 mL of each) were prepared by combining 1.7 mg benzoic acid and 5.7 mg sodium benzoate in 0.5 mL D_2O, to give a 1:3 ratio of acid to Na^+ forms. Two ligand-exchange reactions were then carried out in parallel by adding 50 mg of Na_{34}**1** (1.81 μmol, 3.61 mM) to 0.5 mL of the 0.1 M benzoate buffer solutions in 4 mL vials containing a small magnet to provide mixing. The vials were then placed in a 65 °C oil bath for 18 h. One of the solutions was then transferred to a thin-walled 5-mm precision NMR tube and ^1H and ^{13}C NMR spectra were acquired. The second solution was concentrated to dryness by rotary evaporation in warm (40 °C) water to give a dark red-brown solid. IR: 1617 (m), 1522 (m), 1410 (m), 975 (m), 938 (m), 858 (m), 803 (s), 731 (s), 572 (s) cm^{-1}. Raman: 943 (m), 882 (s) $\nu_{Mo=O}$, ~843 (sh), 370 (s), 311 (m), 212 (m) cm^{-1}. The UV−vis spectrum shows a broad intense band with a maximum at 455 nm. H-1 NMR (400 MHz, D_2O; referenced to HDO at 4.65 ppm relative to external tetramethylsilane): δ = 7.74, 7.43, 7.35 (m, $C_6\boldsymbol{H}_5COO^-$ in bulk solution), 7.2−5.25 (broad, internally coordinated $C_6\boldsymbol{H}_5COO^-$), 1.84 (s, $C\boldsymbol{H}_3COO^-$ in bulk solution), −1.5−0.85 ppm (broad, internally coordinated $C\boldsymbol{H}_3COO^-$). C-13 NMR (400 M Hz, D_2O; referenced to external tetramethylsilane): δ = 179.3 (s, $CH_3\boldsymbol{C}OO^-$ in bulk solution), 174.6 (s, $C_6H_5\boldsymbol{C}OO^-$ in bulk solution), 134.8, 131.6, 128.8, 128.2 (s, $\boldsymbol{C}_6H_5COO^-$ in bulk solution), 125.6 (broad, internally coordinated $\boldsymbol{C}_6H_5COO^-$), 21.9 ppm (s, $\boldsymbol{C}H_3COO^-$ in bulk solution).

Reaction of MTBE with Na_{37}1$(CH_3CO_2)_{13}(C_6H_5CO_2)_{12}$. MTBE (15 μL, 91 μmol) was added directly to an NMR tube containing the benzoate-ligand substituted capsule, prepared as described immediately above. Then, the NMR tube was flame-sealed under air and kept in an oil bath at 65 °C for 23 h, 40 min. H-1 NMR spectra were acquired before and after the reaction.

Cleavage of *p*-Dimethoxybenzene (*p*-DMB) to *p*-Methoxyphenol (*p*-MP) and Methanol. 1,4-Dimethoxybenzene (*para*-DMB; 4.5 mg, 32.6 μmol) was added to a solution of 50 mg Na_{34}**1** (1.81 μmol, 3.61 mM) in 500 μL D_2O. After 19 h 30 min at 65 °C, a ^1H NMR spectrum was acquired. Next, 50 μL of a 12.5 M solution of NaOH in D_2O in air were added (to effect the oxidative alkaline hydrolysis of **1**). The color of **1** was discharged, solid products of hydrolysis that formed immediately were removed by centrifugation, and a ^1H NMR spectrum was acquired.

Temperature Dependence of the Rate Constant for MTBE Cleavage. To obtain $\Delta H^{\ddagger}$ and $\Delta S^{\ddagger}$, 150 μL of pure MTBE were added to an NMR tube containing 18.1 μmol of Na_{34}**1** in D_2O (500 mg in 4.850 mL D_2O). After addition, 500 μL of the solution were transferred to the NMR tube, and the tube was flame-sealed under air. An additional four NMR-tube samples were prepared in the same way. The NMR tubes were placed in separate oil baths, kept at constant temperatures of 55 °C, 60 °C, 65 °C, 70 and 75 °C. Proton-NMR spectra were acquired at regular time intervals, which differed depending on the relative rates of MTBE cleavage. Rate constants associated with MTBE cleavage at each temperature were calculated, and activation parameters were derived from the plot of $\ln(k/T)$ vs $1/k$ (i.e., from a linear form of Eyring equation).

Preparation and Reactions of Capsules, 1, With Accessible, Water-Bound Mo(V) Sites. To replace part of the acetate ligands in **1** by H_2O, 10 mL of concentrated Na_{34}**1** (initially with an average of 20.4 acetates inside; 4.5 mM in water) were placed in a dialysis membrane bag, and immersed in 0.5 L of 0.1 mM methanesulfonic acid (MSA) at pH 4. The slight acidity was used to keep the pH at a value close to the native pH of Na_{34}**1** in water, thus preventing hydrolytic decomposition. The 0.1 mM MSA was replaced by fresh MSA solutions four times over a 10-h period, during which (after 3, 7, and 10 h), aliquots of the solution were drawn from the membrane bag, and dried by rotary evaporation to a dark red-brown solid. These were quantitatively dissolved in D_2O (50 mg in 500 μL) containing an internal MSA integration standard, and ^1H NMR spectra were acquired. After 3, 7, and 10 h, 18.2, 14.9, and 11.8 equiv. of acetate were found inside the capsule, respectively.

For the molybdenum-site dependence study, 100 mg (3.62 μmol) of each acetate/water capsule (20.4, 18.2, 14.9, and 11.8 equiv. of internally bound acetate) were dissolved in 970 μL of D_2O, followed by 30 μL of pure MTBE to achieve total volumes of 1000 μL (3.61 mM **1**). Then, 500 μL of each solution were transferred to an NMR tube, which was flame-sealed and placed in a 65 °C. Proton-NMR spectra were acquired at regular time intervals, which differed depending on the relative rates of MTBE cleavage.

Preparation and Reactions of Capsules, 1, With Inaccessible, Acetate-Blocked Mo(V) Sites. To four separate vials each containing 200 mg (7.24 μmol) of Na_{34}**1** in 1840, 1860, 1908, and 1924 μL of D_2O, 100, 80, 32, and 16 μL (respectively) of aqueous acetate buffer solution (1:1 Na^+: H^+ forms; 4.5 M; pH = 4.7) were added to achieve, in each case, a total volume of 1940 μL (3.73 mM **1**). Then, 500 μL of each solution were transferred to an NMR tube, and NMR spectra were acquired using an external (coaxial) integration standard to quantify the numbers of acetate ligands inside each capsule. The integration standard indicated that 26, 24.4, 23.7, and 22.6 acetates, respectively, were bound inside **1**.

To determine the dependence of rate constants on the number of available (water-occupied) $\{Mo^{V}_2\}$ linkages, 970 μL of each of the 4 solutions described above were transferred to separate vials, and 30 μL of pure MTBE were added to give a total volume of 1000 μL (3.61 mM **1**). Then, 500 μL of each solution were transferred to an NMR tube, flame-sealed, and placed in a constant-temperature 65 °C oil bath. Proton-NMR spectra were acquired at regular time intervals, based on the relative rates of MTBE cleavage in each NMR-tube reaction.

Formation of 3-Methoxy-3-methyl-1-butanol from 3-Methyl-3-butene-1-ol and MeOH. 3-Methyl-3-butene-1-ol, 20 μL (0.198 mmol) and 20 μL (0.494 mmol) of MeOH were added to an NMR tube containing 1.81 μmol of Na_{34}**1** in D_2O (50 mg in 500 μL D_2O, 3.61 mM). The NMR tube was closed tightly, and an ^1H NMR spectrum was acquired 7 min after the addition. The NMR tube was then kept in a 65 °C oil bath for 65 h, and a second ^1H NMR spectrum was acquired.

■ ASSOCIATED CONTENT

Ⓢ Supporting Information

Computational details; spectroscopic, analytical, and computational data; and discussion. This material is available free of charge via the Internet at http://pubs.acs.org.

■ AUTHOR INFORMATION

Corresponding Author

iraw@bgu.ac.il

Notes

The authors declare no competing financial interest.

■ ACKNOWLEDGMENTS

I.A.W. and A.M. thank the Deutsche Forschungsgemeinschaft, for support, Prof. William H. Casey for estimates of water-exchange rates, and Dr. Pere Miro for graphics. C.B. thanks the MINECO of Spain (CTQ2011-29054-C02-02/BQU) and the ICIQ Foundation for support. Dedicated to Prof. Adam Bielanski on the occasion of his 100th birthday.

■ REFERENCES

(1) For *lists* of review articles, see: (a) Amouri, H.; Desmarets, C.; Moussa, J. *Chem. Rev.* **2012**, *112*, 2015−2041. (b) Chakrabarty, R.; Mukherjee, P. S.; Stang, P. J. *Chem. Rev.* **2011**, *111*, 6810−6918.

(2) For leading refs by many authors: (a) Laughreya, Z.; Gibb, B. C. *Chem. Soc. Rev.* **2011**, *40*, 363−386. (b) Wiester, M. J.; Ulmann, P. A.; Mirkin, C. A. *Angew. Chem., Int. Ed.* **2011**, *50*, 114−137. (c) Yoshizawa, M.; Fujita, M. *Bull. Chem. Soc. Jpn.* **2010**, *83*, 609−618. (d) Yoshizawa, M.; Klosterman, J. K.; Fujita, M. *Angew. Chem., Int. Ed.* **2009**, *48*, 3418−3438. (e) Pluth, M. D.; Bergman, R. G.; Raymond, K. N. *Acc. Chem. Res.* **2009**, *42*, 1650−1659. (f) Ajami, D.; Rebek, J. *Top. Curr. Chem.* **2012**, *319*, 57−78.

(3) (a) Todea, A. M.; Merca, A.; Bögge, H.; van Slageren, H. J.; Dressel, M.; Engelhardt, L.; Luban, M.; Glaser, T.; Henry, M.; Müller, A. *Angew. Chem., Int. Ed.* **2007**, *119*, 6218−6222. (b) Sadakane, M.; Yamagata, K.; Kodato, K.; Endo, K.; Toriumi, K.; Ozawa, Y.; Ozeki, T.; Nagai, T.; Matsui, Y.; Sakaguchi, N.; Pyrz, W. D.; Buttrey, D. J.; Blom, D. A.; Vogt, T.; Ueda, W. *Angew. Chem., Int. Ed.* **2009**, *48*, 3782−3786.

(4) (a) Ziv, A.; Grego, A.; Kopilevich, S.; Zeiri, L.; Miro, P.; Bo, C.; Müller, A.; Weinstock, I. A. *J. Am. Chem. Soc.* **2009**, *131*, 6380−6382. (b) Petina, O.; Rehder, D.; Haupt, E. T. K.; Grego, A.; Weinstock, I. A.; Merca, A.; Bögge, H.; Szakacs, J.; Müller, A. *Angew. Chem., Int. Ed.* **2011**, *50*, 410−414. (c) Schäffer, C.; Bögge, H.; Merca, A.; Weinstock, I. A.; Dieter Rehder, D.; Haupt, E. T. K.; Müller, A. *Angew. Chem., Int. Ed.* **2009**, *48*, 8051−8046. (d) Schäffer, C.; Todea, A. M.; Bögge, H.; Petina, O. A.; Rehder, D.; Haupt, E. T. K.; Müller, A. *Chem.—Eur. J.* **2011**, *17*, 9634−9639.

(5) Polydore, C.; Roundhill, D. M.; Liu, H.-Q. *J. Mol. Cat. A.* **2002**, *186*, 65−68.

(6) On the basis of data in ref 4c showing that heating dramatically affects ligand exchange, the entry of benzoate (ref 4a) was revisited. After 24 h at 65 °C, and using the Na^+-salt (more soluble than the acid form used earlier)—benzoate is indeed observed inside **1** (see SI).

(7) (a) Breno, K. L.; Ahmed, T. J.; Pluth, M. D.; Balzarek, C; Tyler, D. R. *Coord. Chem. Rev.* **2006**, *250*, 1141−1151. (b) This is difficult to quantify more precisely because observed pD values result from the dissociation of protons from multiple water ligands on numerous $\{Mo^{V}_{2}\}$ linkages.

(8) Accordingly, the intensity ratio of ^{1}H NMR signals of *tert*-BuOD "$(CH_3)_3C$-" and methanol "-CH_3" groups after MTBE cleavage in D_2O was 8:3, smaller than the 9:3 ratio for unreacted MTBE.

(9) Blackmond, D. G. *Angew. Chem., Int. Ed.* **2009**, *48*, 2648−2654.

(10) Bielanski, A.; Lubanska, A.; Micek-Ilnicka, A.; Pozniczek, J. *Coord. Chem. Rev.* **2005**, *249*, 2222−2231.

(11) (a) Richens, D. T. *Chem. Rev.* **2005**, *105*, 1961−2002. (b) William H. Casey, private communication.

(12) Catalytic cycles involving a single Mo(V) center—whether as a Lewis acid, or with a bound water ligand acting as a Brønsted acid—require the inclusion of elementary steps whose microscopically reverse processes appear much less plausible (see Figures S17 and S18 of the SI).